

# Capabilities of GaN/AlN/GaN structures as high-intensity pyroelectric laser sensors

E.A. Panyutin, M.L. Shmatov

**Abstract.** The use of transparent  $\text{Al}_2\text{O}_3/\text{GaN}/\text{AlN}/\text{GaN}$  structures as pyrometric sensors for measuring the parameters of high-intensity laser pulses is proposed. The peculiarities of the employment of such sensors in laser fusion facilities are analysed. Post-pulse distributions of the absorbed energy density are obtained for various parameters of both GaN layers. The local maxima of these distributions are minimised by varying the ratio of donor concentration and the ratio of their thicknesses under the condition of invariance of the total absorbed energy. The optimal structure configuration is established in terms of reducing the possible negative effect of laser impact on the pyroelectric coefficient stability.

**Keywords:** laser thermonuclear fusion, aluminium nitride, pyroelectric effect.

## 1. Introduction

Among various fields of application of high-power pulsed lasers (for example, laser technologies, remote sensing and laser-plasma accelerators), the laser approach to the problem of obtaining a controlled fusion reaction is the most relevant. Therefore, the research and development focused on the development of new means for recording the laser pulse parameters, with allowance for the problem specificity, also seem important.

Laser initiation of thermonuclear microexplosion requires both a high flux of radiation energy density, which can currently be achieved using multichannel laser facilities, and fulfilling a set of conditions to ensure the efficient conversion of this energy into the internal energy of the fuel. The efficiency of the conversion and, as a consequence, the efficiency of a laser thermonuclear target largely depends on the homogeneity of the profiles of individual laser beams used for the target irradiation [1–5]. First and foremost, this refers to the compression of targets in direct initiation schemes, which require high uniformity of ablator irradiation [3, 4]. At the same time, the presence of a certain inhomogeneity of the beam is even useful for the generation of hot electrons in some proposed variants of shock ignition [5], as well as for the implementation of several scenarios of fast ignition [6, 7].

To optimise the laser beam profiles, direct radiation recording is desirable, which allows one to avoid nonlinear

distortions when radiation is attenuated. This imposes special requirements on the basic materials of the sensors in terms of their thermo-mechanical parameters, allowing multiple operation of the sensor in the course of radiation heating to a temperature of at least 1000 °C.

For example, in the UFL-2M facility (192 amplification channels with a beam aperture of  $40 \times 40$  cm and a pulse duration of 3–5 ns), the multi-pulse energy at a wavelength  $\lambda = 1.06 \mu\text{m}$  (i.e., before the generation of the second harmonic with  $\lambda = 0.53 \mu\text{m}$  directly affecting the target) is 4.6 MJ [8, 9]. Accordingly, the radiation energy density flux of a single channel is  $q \sim 15 \text{ J cm}^{-2}$  and the intensity  $I(t)$  reaches  $\sim 3 \text{ GW cm}^{-2}$ , which provides a basis for the formulation of the task of developing sensors with the lowest possible energy absorption, i.e. transparent to the radiation of both the fundamental frequency and the harmonic used. One of the possible approaches to solving the problem of determining the local parameters of high-intensity beams is the use of the pyroelectric effect implemented in semiconductor structures based on materials having a suitable type of crystal lattice, as example, broadband III-nitrides, for which the means and methods of microlithography are applicable.

## 2. Problem statement

The use of the pyroelectric effect for laser radiometry problems has long been known, and until recently sensitive sensor elements have been designed based on the nontransparent ceramic pyromaterials (see, for example, [10, 11] and references therein). However, due to the development of GaN and AlN epitaxial technologies, including HVPE technology [12], increased attention was paid to the study of similar effects in these materials. Aluminium nitride is a broadband (band gap  $E_g = 5.9 \text{ eV}$ ) semiconductor and, having a lattice of hexagonal symmetry (wurtzite structure), is characterised by the presence of a selected  $c$  axis, which implies the presence of built-in electrical polarisation, as well as its change with a change in the lattice temperature, i.e. pyroelectric effect.

Experimental confirmation of the presence of the pyroelectric effect in aluminium nitride [13], and also the subsequent study of its characteristic features for a bulk monocrystalline material [14, 15], has shown that, as expected, the pyroelectric response in this case is somewhat inferior to the similar value typical of ferroelectric pyroelectrics. Recently, a study was conducted of the pyroelectric effect in an epitaxial AlN-layer grown by the HVPE method on an electrically conductive SiC substrate supplemented with metal contacts; a laser with wavelength  $\lambda = 0.98 \mu\text{m}$  and pulse energy  $\sim 0.1 \text{ J}$  was used for excitation. The pyroelectric signal measurement for such structures [16] and subsequent calculation of the

E.A. Panyutin, M.L. Shmatov Ioffe Institute, Russian Academy of Sciences, Polytekhnicheskaya ul. 26, 194021 St. Petersburg, Russia; e-mail: eugeny.panyutin@mail.ioffe.ru

Received 25 November 2018; revision received 30 July 2019  
*Kvantovaya Elektronika* 49 (11) 1078–1082 (2019)  
Translated by M.A. Monastyrsky

pyroelectric coefficient showed that its values lie in the range  $(2.5\text{--}6) \times 10^{-6} \text{ C m}^{-2} \text{ K}^{-1}$ , which is about an order of magnitude smaller than the values of the pyroelectric coefficients for ferroelectrics of the LiTaO<sub>3</sub> or TGS type; however, this circumstance is obviously not decisive for the detection of high-intensity pulses.

More significant is the possibility of obtaining the GaN/AlN/GaN multilayer structures with gallium nitride ( $E_g = 3.39 \text{ eV}$ ) in a single technological cycle in the form of n-type layers (of thickness  $1\text{--}50 \text{ }\mu\text{m}$ ) with a concentration  $n_c$  of free electrons, directly determined by the donor concentration  $N_d$  ( $n_c \sim N_d$ ) which is well-controlled in the range of  $10^{17}\text{--}10^{19} \text{ cm}^{-3}$ . Such layers, having sufficient, though significantly lower than that of AlN, transparency for radiation with  $\lambda > 0.36 \text{ }\mu\text{m}$  and, at the same time, characterised by high electrical conductivity (GaN electron mobility  $\mu_n = 200\text{--}1000 \text{ cm}^2 \text{ V}^{-1} \text{ s}^{-1}$ ), can serve as transparent electrodes. In this regard, it seems appropriate to study the features of energy absorption and heating of such a multilayer structure, as well as the possibility of optimising the structural and technological parameters of the structure from the viewpoint of reducing its maximum local temperature.

### 3. Modelling and discussion of results

Since the main contribution to the absorption of light in the electrode GaN layers is made by its interaction with free carriers, the absorption at these wavelengths can be estimated by the classical formula for the absorption coefficient  $\alpha_n$  on free electrons

$$\alpha_n = G_n \frac{\sigma}{n_{\text{ref}} (\omega \tau_m)^2} \quad (1)$$

( $G_n = 377$ ;  $\sigma$  is the specific conductivity;  $n_{\text{ref}}$  is the refractive index;  $\omega$  is the frequency of light; and  $\tau_m$  is the relaxation time of the ensemble of electrons by momentum [17]), which can be presented in a somewhat different form, more convenient for further use:

$$\alpha_n = G_0 (\lambda^2 n_e) / \mu_n, \quad (2)$$

where  $G_0 = e^3 / (4\pi^2 \epsilon_0 c^3 m_n^* n_{\text{ref}})$ ;  $e$  is the electron charge;  $\epsilon_0$  is the electric constant;  $c$  is the speed of light; and  $m_n^*$  is the effective electron mass in GaN, determined through a free electron mass  $m_e$  ( $m_n^* = 0.19 m_e$ ). Hence, the constant  $G_0$  for GaN in the ESU units takes the value  $6.072 \times 10^{-8}$  (see also [18]).

Since the pulsed heating of a crystal lattice is directly related to the amount of absorbed light energy, temperature distributions can be obtained based on the general information provided by the light absorption laws (it is sufficient to consider the case of spatial scales exceeding  $\lambda$ ) and information regarding the thermophysical parameters of the material, which is of undoubted practical interest.

The light energy absorbed by the medium as the beam travels the path  $z$  is defined as  $B(z) = A_0 - A(z)$ , where  $A_0$  is the input flux intensity; and  $A(z)$  is the value corresponding to its decrease with increasing  $z$ . For a homogeneous medium (exponential decay), the absorbed light energy density has the form

$$p(z) = dB(z)/dz \equiv A_0 \alpha_n \exp(-\alpha_n z). \quad (3)$$

In the case of adiabatic character of heat release (the pulse exposure time is much less than the characteristic times of heat redistribution and convective exchange with the air), the

temperature profile  $T(z)$  during the beam action retains its shape after the pulse termination and qualitatively coincides with the absorbed energy density distribution  $p(z)$ . In the simplest case, when all parameters can be considered independent of the coordinate and temperature, obtaining such a distribution, formed at the termination of light exposure, is reduced to solving the heat balance equation  $\Delta T(z) m C_v = A_0 \alpha_n \exp(-\alpha_n z)$ , where

$$\Delta T(z) = [A_0 \alpha_n / (m C_v)] \exp(-\alpha_n z). \quad (4)$$

Here  $\Delta T$  is the temperature change during the pulse action;  $C_v$  is the specific heat capacity of the material; and  $m$  is the mass of the object. However, for high-intensity light pulses, obviously, one should make allowance for the possibility of temperature dependence of some parameters included in the balance equation. Directly for the GaN layers that are to be subjected to the greatest thermal effects, this applies to both the specific heat capacity  $C_p$  and  $\alpha_n$ . The absorption coefficient is temperature-dependent primarily through the electron mobility  $\mu_n$ , which (at  $T \gtrsim 250 \text{ K}$ ) increases with temperature due to an increase in the contribution of scattering on optical phonons [19] and, in the range of  $20\text{--}500 \text{ }^\circ\text{C}$ , can be approximated by the formula  $\mu_n(T) = \mu_{n0} + \mu_{n1} T$ , where  $\mu_{n0} = 400$  and  $\mu_{n1} = -0.55$ . Given that the absorption coefficient is  $\alpha_n(T) \sim \mu_n(T)^{-1}$ , after expanding  $\alpha_n(T)$  into a Taylor series and restricting ourselves to linear terms, we obtain  $\alpha_n(T) = \alpha_{n0} + \alpha_{n1} T$ , where  $\alpha_{n0} = G_0 (\lambda^2 N_d) / \mu_{n0}$  and  $\alpha_{n1} \approx 10^{-2} \alpha_{n0}$ .

As for the specific heat capacity  $C_p$ , according to the latest experimental data [20, 21] it depends on the temperature in a sophisticated way, so that the approximation of this value by a polynomial curve with the preservation of the first terms and subsequent transformation leads to the expression (in  $\text{J g}^{-1} \text{ }^\circ\text{C}^{-1}$ )

$$C_p(T) \simeq C_{p0} + C_{p1} T,$$

where  $C_{p0} = 0.41$  and  $C_{p1} = 3.06 \times 10^{-4}$ . Using the resulting expression, given that now  $B(z) \equiv B(T(z))$ , the heat balance equation for an area of  $1 \text{ cm}^2$  can be represented as follows:

$$\begin{aligned} \Delta T(z) \rho d (C_{p0} + C_{p1} \Delta T(z)) &= A_0 \exp\{-[\alpha_{n0} + \alpha_{n1} \Delta T(z)]z\}, \\ &\times \{\alpha_{n0} + \alpha_{n1} [\Delta T(z) + z d \Delta T(z) / dz]\}, \end{aligned} \quad (5)$$

where  $\rho$  is the density and  $d$  is the layer thickness.

This equation, in turn, is a differential equation for  $d\Delta T/dz$  containing a small parameter  $\alpha_{n1}$  at the derivative, i.e. it belongs to the class of singularly perturbed equations, the development of regular methods for solving which is associated with known difficulties. However, for the case of small temperature gradients within a single layer (i.e. at  $(d\Delta T/dz) < T$ ), which corresponds to negligible absorption, differential equation (5) becomes functional:

$$\begin{aligned} \Delta T(z) \rho d (C_{p0} + C_{p1} T(z)) \\ = A_0 \exp\{-[\alpha_{n0} + \alpha_{n1} \Delta T(z)]z\} [\alpha_{n0} + \alpha_{n1} \Delta T(z)]. \end{aligned} \quad (6)$$

After presenting the temperature distribution as

$$\Delta T(z) = \sum_{k=0} T_k z^k,$$

equation (6) can be solved using the method of undetermined coefficients. In particular, restricting ourselves to the first two terms of the expansion with respect to the distribution constants  $T_0$  and  $T_1$ , we arrive at a system of equations

$$T_0^2 + \frac{d\rho C_{p0} - A_0\alpha_{n0}}{d\rho C_{p1}} T_0 + \frac{A_0\alpha_{n0}}{d\rho C_{p1}} = 0, \quad (7)$$

$$T_1^2 + \frac{d\rho C_{p0} - A_0\alpha_{n1}}{d\rho C_{p0}} T_1 + \frac{A_0\alpha_{n1}^2 T_0^2 + \alpha_{n0}^2 + \alpha_{n0}^2}{d\rho C_{p0}} = 0, \quad (8)$$

which relates these constants with the input flow intensity  $A_0$  and material parameters, from which the maximum temperature  $T_{\max}$  in the interval  $[0, d]$  can be derived.

The basic structure of a real sensor must contain at least four optically different layers: an active AlN layer (thickness  $\sim 10 \mu\text{m}$ ,  $\alpha_{\text{AlN}} \approx 10^{-2} - 10^{-1} \text{cm}^{-1}$  [22]), two conductive electrodes (GaN layers having a thickness of 2–50  $\mu\text{m}$ , specific conductivity  $\sigma > 1.0 \Omega^{-1} \text{cm}^{-1}$ , and absorption coefficient  $\alpha_{\text{GaN}} = 1-5 \text{cm}^{-1}$ ), and also a substrate that determines the possibility and character of epitaxial growth.

Due to the rather strict limitations imposed on the crystallographic parameters of the substrate material during the GaN epitaxial growth, as well as guided by commercial availability, it is currently possible to use sapphire or SiC substrates; however, the need for high transparency of the substrate unambiguously implies the use of  $\text{Al}_2\text{O}_3$  ( $\alpha_{\text{Al}_2\text{O}_3} \sim 10^{-2} \text{cm}^{-1}$ ) [23].

Leucosapphire and aluminium nitride in the form of monoplates allow a very intense laser action and, possess, according to experimental data, a high damage threshold (200–400  $\text{GW cm}^{-2}$  for a pulse of 10 ns duration at  $\lambda = 1.06 \mu\text{m}$  [24]), which is two orders of magnitude higher than the peak intensity value of the pulses considered in this work. However, multilayer heterostructures are characterised by uneven heat release: pulse heating of less transparent GaN layers can lead to a rapid increase in their temperature by hundreds of degrees; in this case, the heating of the AlN layer at the pulse end is about an order of magnitude less. As a result, the development of internal (mainly tangential) stresses is possible, caused not only by large temperature gradients, but also by the difference in thermal expansion coefficients of materials of adjacent layers ( $\delta_{\text{Al}_2\text{O}_3} = 7.2 \times 10^{-6} \text{K}^{-1}$ ,  $\delta_{\text{GaN}} = 5.7 \times 10^{-6} \text{K}^{-1}$ ,  $\delta_{\text{AlN}} = 4.03 \times 10^{-6} \text{K}^{-1}$ ). These stresses can reach a noticeable value near the interface planes and, given the elevated temperature, provoke the generation and accumulation of dislocations.

Although the equilibrium (technological) temperature of the structure formation is approximately 1050–1100  $^\circ\text{C}$ , and its subsequent cooling to  $T = 20^\circ\text{C}$  results in elastic stresses, this does not lead to the development of destructive processes at these layer thicknesses. Nevertheless, in order to smooth out the light dynamic shocks and reduce their negative impact on the pyroelectric coefficient stability, it is reasonable to consider and analyse possible ways to reduce such stresses, determined mainly by the heat release in gallium nitride.

In this regard, and with allowance for the presence of some technological freedom with respect to the thickness of epitaxial layers and the level of GaN doping, it is desirable to have at least an assessment of the optimal configuration of the structure in terms of minimising the maximum temperature and its gradient at the AlN layer boundaries under the condition of invariance of the pulse energy.

Due to the layered structure of the sensor, the distribution  $p(z)$  of absorbed energy density can be conveniently described by a set of parameters  $p_j$  – densities of energy absorbed within the  $j$ th layer. In the case illumination comes from the side of the  $\text{Al}_2\text{O}_3$  substrate, a model that accounts for reflections from the boundaries and neglects higher-order reflexes along with the effects of multipath interference leads in a linear approximation to an expression describing the superposition of absorption of forward and reflected waves:

$$P_j(z) = A_j \alpha_j (1 - R_i) \exp(-\alpha_j z) + A_{i+1} R_{i+1} \exp(\alpha_j (d_j - z)), \quad z_i \leq z < z_{i+1}. \quad (9)$$

Here  $j$  is the layer number;  $i$  is the boundary number (including the boundaries with the air environment); the coordinates  $z_i$  are determined through the thickness  $d_j$  of the  $j$ th layer as  $z_{i+1} = z_i + d_j$  (in our case, the four-layer system  $j = 1 - 4$  and  $i = 1 - 4$ );  $A_j$  is the input light flux; and  $R_j$  is the reflection coefficient, which is calculated from the Fresnel equations and, in the case of normal incidence, takes the form

$$R_i = (n_{j+1} - n_j) / (n_{j+1} + n_j).$$

In this situation, the values of optical parameters of the layers are distributed as follows:

$$\alpha_j \in \{\alpha_{\text{Al}_2\text{O}_3}, \alpha_{\text{GaN1}}, \alpha_{\text{AlN}}, \alpha_{\text{GaN2}}\},$$

$$n_j \in \{n_{\text{Al}_2\text{O}_3}, n_{\text{GaN1}}, n_{\text{AlN}}, n_{\text{GaN2}}, 1\}$$

(values of refraction coefficients are as follows:  $n_{\text{Al}_2\text{O}_3} = 1.77$ ,  $n_{\text{GaN1}} = n_{\text{GaN2}} = 2.40$ ,  $n_{\text{AlN}} = 2.30$ ; for an air environment,  $n_{\text{air}} = 1$ ; in addition,  $\alpha = 0$ ).

For normalisation constants, the calculation of which is necessary to ensure the light flux continuity, in the approximation of the reflections of small multiplicity, the following recurrence relation can be obtained:

$$A_{i+1} = A_i \exp[-(\alpha_{j+1} - \alpha_j) z_{i+1}] + R_{i+1} A_i \exp[(\alpha_{j+1} - \alpha_j)(d_j - z_{i+1})]. \quad (10)$$

Next, applying a procedure similar to that used in the derivation of Eqns (7) and (8), we can obtain temperature distributions  $T(z)$  and distributions of the absolute value of gradients  $|\text{grad}T(z)|$ , from which, in turn, we find values of both local (within a single layer) maxima of  $T_{\max j}$  and  $|\text{grad}T|_{\max j}$ , and also global maxima of  $T_{\max}$  and  $|\text{grad}T|_{\max}$ .

Since  $\min(\alpha_{\text{GaN1}}, \alpha_{\text{GaN2}}) > \max(\alpha_{\text{Al}_2\text{O}_3}, \alpha_{\text{AlN}})$ , the nature of the greatest heat release is determined mainly by the properties of the GaN layers. In the simplest case, when the relations between the parameters (thicknesses  $d$  and concentrations  $N_d$ ) of both layers are intentionally not taken into consideration, the dependence of the temperature  $T_{\max}$  on the average doping level of  $N_{d \text{ GaN}}$  [here  $N_{d \text{ GaN}} = (N_{d \text{ GaN1}} N_{d \text{ GaN2}})^{1/2}$ ] for various values of  $A_0$  of the input flux is shown in Fig. 1. The superlinear character of these curves, which dominates at modest temperatures and is obviously stipulated by a decrease in the mobility of electrons, is gradually replaced by a dependence being more close to linear. It is assumed that this is due to the influence of the compensating effect of temperature-dependent heat capacity. A typical view of the temperature distribution is shown in the inset to this Figure.

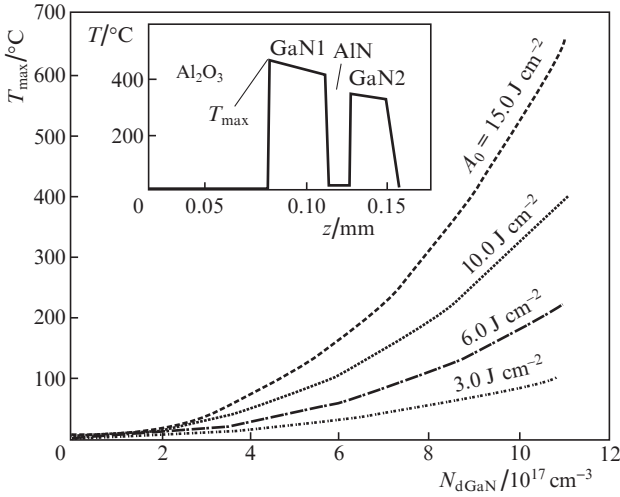


**Figure 1.** Temperature in the plane of maximum heat release as a function of the doping level of GaN layers for various energy densities of the input radiation flux. The inset shows a typical post-pulse temperature distribution  $T(z)$  over the thickness of a four-layer structure.

Since epitaxial technologies make it relatively easy to control not only the thickness of the GaN layers, but also (within the above limits) the level of their doping, it is advisable to consider the possibility of finer tuning of the distribution shape in order to decrease the  $T_{\max}$  value at the same intensity value  $A_0$  of the output light flux.

Although this optimisation is limited to varying the properties of only GaN electrodes, the total number of parameters that can be independently changed (namely,  $d_{\text{GaN1}}$ ,  $N_{\text{dGaN1}}$ ,  $d_{\text{GaN2}}$  and  $N_{\text{dGaN2}}$ ) cannot be considered small. At the same time, it is obvious that a reasonable reduction in their number is possible as a result of the allocation of the most significant directions in the corresponding 4D space, which requires the introduction of a new system of parameters. In particular, while the effective  $N_{\text{dGaN}}$  concentration makes it possible to estimate only the averaged energy absorption, the variation of the coefficient  $K_N = N_{\text{dGaN1}}/N_{\text{dGaN2}}$  under the condition of  $N_{\text{dGaN}}$  invariance allows for a more detailed study of temperature distributions. In addition, guided by considerations of ensuring a reasonable duration of the technological process for any allowable configuration of layers, it is expedient to impose the invariance condition on the total thickness  $d_{\text{GaN}} = d_{\text{GaN1}} + d_{\text{GaN2}}$ , which allows us to effectively describe the geometry change of the structure by means of parameter  $K_d = d_{\text{GaN2}}/d_{\text{GaN1}}$ .

Based on the above reasoning, we constructed an algorithm in MATLAB to calculate the corresponding distributions along the beam of absorbed energy density (temperature distributions) and their gradients. The dependences shown in Fig. 2, obtained for the energy density of the input flux  $A_0 \sim 15\text{ J cm}^{-2}$  and the average doping level  $N_{\text{dGaN}} = 9.73 \times 10^{17}\text{ cm}^{-3}$  (which limits  $T_{\max}$  to 500–600 °C) demonstrate the presence of sharp minima. Curves reflecting the behaviour of  $T_{\max}$  and the moduli of the gradient  $|\text{grad}T|_{\max}$  at the points of its minimum with respect to  $K_N$  when varying  $K_d$  at  $d_{\text{GaN}} = 44\text{ }\mu\text{m}$  and  $A_0 \sim 15\text{ J cm}^{-2}$  (Fig. 3) have, on the contrary, a monotonic character.

Further evolution of the thermal field corresponding to the microsecond and millisecond ranges consists in temperature redistribution and gradual heating of the active pyroelectric AlN layer. As a result, this heating leads to the appear-

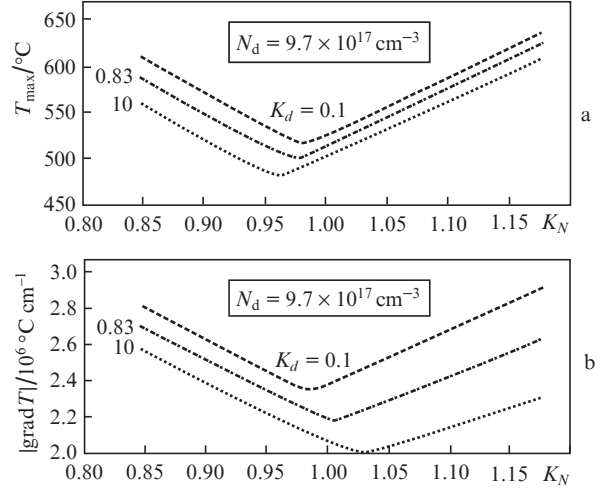


**Figure 2.** Dependence of local maxima of (a) temperature  $T(z)_{\max}$  and (b) gradient modulus  $|\text{grad}T(z)|_{\max}$  on the concentration ratio of donors  $K_N = N_{\text{dGaN1}}/N_{\text{dGaN2}}$  in GaN layers for different  $K_d$  values. The energy density of the input light flux is  $\sim 15\text{ J cm}^{-2}$ .

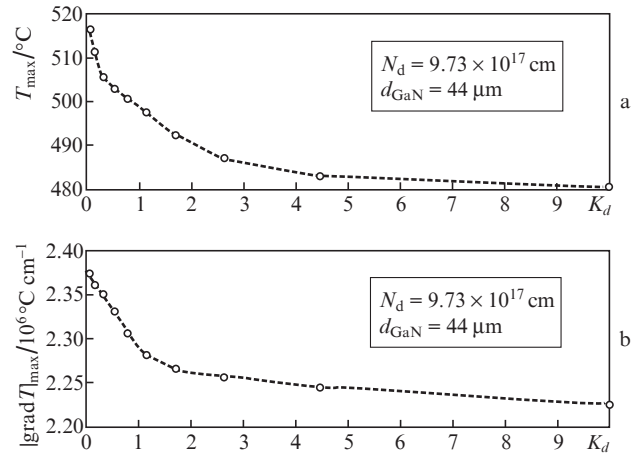


**Figure 3.** Minimum values (see Fig. 2) of local maxima of (a) temperature  $T_{\max}$  and (b) gradient modulus  $|\text{grad}T|_{\max}$  on the ratio of the thicknesses of GaN layers. The energy density of the input light flux is  $\sim 15\text{ J cm}^{-2}$ .

ance of an electric signal on the GaN electrodes. The dynamics of this response in a rather sophisticated way (through a time-dependent pyroelectric coefficient) is associated with changes in temperature and absorbed energy, since it depends, among other things, on the thermophysical parameters of a particular structure, and is the subject of an independent research area [10, 16]. However, if we are only interested in the relative values of the pyroelectric coefficient (the case of transverse homogeneity of the beam), the issue of their relationship with the geometry and heat transfer characteristics of a particular sensor structure ceases to be relevant.

Since the pyroelectric response values in AlN layers, recorded earlier for pulses (microvolt range) with an energy of  $\sim 0.1\text{ J}$ , when illuminating the area  $S = 0.2\text{ cm}^2$  at 100% light absorption, provided an accuracy of temperature measurement of no lower than 0.1 K [13, 16], it can be assumed that similar values of the signal level for fluxes with a density of 10–15  $\text{J cm}^{-2}$  can be implemented in sensors with a significantly smaller active element area. It should be noted that the

possibility of using transparent materials (in particular, SiO<sub>2</sub>) for similar purposes has been discussed earlier [25]. However, since microlithography is an organic and well-grounded method for the proposed semiconductor structures, arrays of multi-element pyrometric sensors can be developed and manufactured on their basis, the length of which in a single-chip design is limited mainly by the substrate sizes and can currently reach 50–60 mm.

#### 4. Conclusions

Based on the foregoing, we can conclude that transparent or partially transparent epitaxial GaN/AlN/GaN structures obtained on transparent sapphire substrates by the HVPE method, which provides the possibility of deposition of layers over a wide range of thicknesses, can be used for post-epitaxial formation of mono- or multielement pyroelectric sensors for recording the energy density of fluxes, as well as energy distribution over the beam cross section, up to integral values of 15 J cm<sup>-2</sup> and higher. An additional reason for the expediency of using these materials is their exceptional heat resistance and thermal stability. However, unlike traditional pyroelectric sensors, the characteristic feature of which is the complete absence of spectral dependence, the sensor structures considered are spectrally dependent, which should be taken into account when developing sensor elements.

#### References

- Lindl J. *Phys. Plasmas*, **2**, 3933 (1995).
- Pennington D.M., Henessian M.A., Wilcox R.B., Weiland T.L., Eimerl D. *Inert. Conf. Fusion*, **5** (2), 130 (1995).
- Radha P.B., Hohenberger M., Edgell D.H., et al. *Phys. Plasmas*, **23**, 056305 (2016).
- Peebles J.L., Hu S.X., Theobald W., Goncharov V.N., Whiting N., Celliers P.M., Ali S.J., Duchateau G., Campbell E.M., Boehly T.R., Regan S.P. *Phys. Rev.*, **99**, 063208 (2019).
- Llor Aisa E., Ribeyre X., Duchateau G., Nguyen-bui T., Tichonchuk V.T., Colaïtis A., Betti R., Bose A., Theobald W. *Phys. Plasmas*, **24**, 112711 (2017).
- Shmatov M.L. *Fusion Sci. Technol.*, **43**, 456 (2003).
- Atzeni S., Tabak M. *Plasma Phys. Contr. Fusion*, **47**, B769 (2005).
- Garanin S.G. *Phys. Usp.*, **54**, 415 (2011) [*Usp. Fiz. Nauk*, **181**, 435 (2011)].
- Garanin S.G., Belkov S.A., Bondarenko S.V. *Proc. XXXIX Int. Conf. on Plasma Physics and Controlled Fusion (Zvenigorod, 2012)*.
- Aleksandrov S.E., Gavrilov G.A., Kapralov A.A., Smirnova E.P., Sotnikova G.Yu., Sotnikov A.V. *Zh. Tekh. Fiz.*, **74** (9), 72 (2004).
- Aleksandrov S.E., Gavrilov G.A., Kapralov A.A., Muratkov K.L., Sotnikova G.Yu. *Tech. Phys. Lett.*, **43** (12), 1084 (2017) [*Pis'ma Zh. Tekh. Fiz.*, **43** (23), 77 (2017)].
- Bessolov V.N., Konenkova E.V., Kukushkin S.A., Nikolaev V.I., Osipov A.V., Sharofidinov Sh.Sh., Shcheglov M.P. *Pis'ma Zh. Tekh. Fiz.*, **39** (6), 1 (2013).
- Bukhovski A.D., Kaminski V.V., Shur M.S., Chen Q.C., Khan M.A. *Appl. Phys. Lett.*, **69** (21), 3254 (1996).
- Shaldin Yu.V., Matiasik S. *Fiz. Tekh. Poluprov.*, **45** (9), 1159 (2011).
- Kukushkin S.A., Osipov A.V., Sergeeva O.N., Kiselev D.A., Bogomolov A.A., Solnyshkin A.V., Kaptelov E.Yu., Senkevich S.V., Pronin I.P. *Phys. Solid State*, **58** (5), 967 (2011) [*Fiz. Tverd. Tela*, **58** (5), 937 (2016)].
- Gavrilov G.A., Kapralov A.F., Muratkov K.L., Panyutin E.A., Sotnikov A.V., Sotnikova G.Yu., Sharofidinov Sh.Sh. *Tech. Phys. Lett.*, **44** (8), 709 (2018) [*Pis'ma Zh. Tekh. Fiz.*, **44** (16), 1 (2018)].
- Seeger K. *Semiconductor Physics* (Wien, New York: Springer Verlag, 1973; Moscow: Mir, 1977).
- Pankove J.I. *Optical Processes in Semiconductors* (Englewood Cliffs, New Jersey: Prentice-Hall, 1971; Moscow: Mir, 1973).
- Saxler A., Look D.C., Elhamri S., Sizelove J., Mitche W.C., Sung C.M., Parc S.S., Lee K.Y. *Appl. Phys. Lett.*, **78** (12), 1873 (2001).
- Leitner J., Strejc A., Sedmidubsky D., Ruzicka K. *Thermochemical Acta*, **401**, 169 (2003).
- Lee S., Kwon S.Y., Ham H.J. *Jpn. J. Appl. Phys.*, **50**, 11RG02 (2011).
- Blank T.B., Goldberg Yu.A. *Fiz. Tekh. Poluprovodn.*, **37** (9), 1025 (2003).
- Lingart Yu.K., Petrov V.A., Tikhonova N.A. *Teplofiz. Vys. Temp.*, **20** (5), 872 (1982).
- Gorshkov B.G., Epifanov A.S., Manenkov A.A., Panov A.A. *Sov. J. Quantum Electron.*, **6** (11), 2415 (1979) [*Kvantovaya Elektron.*, **9** (11), 1420 (1979)].
- Kosorotov V.F., Shchedrina L.V. *Quantum Electron.*, **40** (3), 271 (2010) [*Kvantovaya Elektron.*, **40** (3), 271 (2010)].